Temperature Dependence of the Pyroelectric Effect in Cadmium Sulfide*

WILFRED J. MINKUS†
The Rome Air Development Center, Griffiss Air Force Base, New York
(Received 1 September 1960; revised manuscript received 21 December 1964)

This paper describes the observed temperature dependence of the pyroelectric effect in a hexagonal cadmium sulfide crystal between 78 and 345°K. The methods used to obtain the response and evaluate the results are described. The error is evaluated at each of the ambient temperatures. The measurements were made along the crystal's axis of symmetry. Most of the polarization appears to be due to the dipole expansion of interatomic bonds which are principally covalent.

1. INTRODUCTION AND EXPERIMENTAL PROCEDURES

WHEN certain types of crystals are heated, they develop a spontaneous polarization along a unique axis. This phenomenon is known as the pyroelectric effect, and the ratio between the amount of polarization produced and the temperature rise of the crystal is known as the pyroelectric constant. The object of the experimental phase of the study was to measure the pyroelectric constant of a hexagonal cadmium sulfide crystal at certain temperatures between 78 and 345°K. The apparatus used in this measurement is shown in Fig. 1. As indicated, the specimen was mounted in a holder which was immersed in a constant-temperature bath. When the crystal was heated a small amount above the ambient, its pyroelectric response was amplified and recorded, and its temperature rise was measured.

The main features of the crystal holder are indicated in Fig. 2. Because cadmium sulfide is photoconductive, the holder had to be designed to maintain the crystal in a light-tight environment. In order to obtain an adequate response level from the small amount of pyroelectric charge, it was required to have an extremely high level of electrical insulation and a low capacitance. Sufficient thermal insulation had to be provided so that the crystal could be heated a small but controllable amount above the ambient temperature.

As indicated in Fig. 2, the crystal holder consisted of the inner holder, the heating coil, the cover, and the connector units. The inner holder was 70 cm in length and constructed almost entirely of thin-walled Monel tubing of 15-mm diameter. The crystal was mounted in the lower portion of the unit and connected between two probes set at opposite ends of its axis of symmetry, the optical axis. The bottom probe was connected to the grounded walls of the unit, and the upper probe was connected to an insulated post at the top of the holder. The thick layer of silver paste used in connecting each end of the specimen to its probe provided a cushion into which it could expand when heated. A heating coil was wound on a brass cylinder and centered about the specimen. A thermocouple was embedded in the cylinder

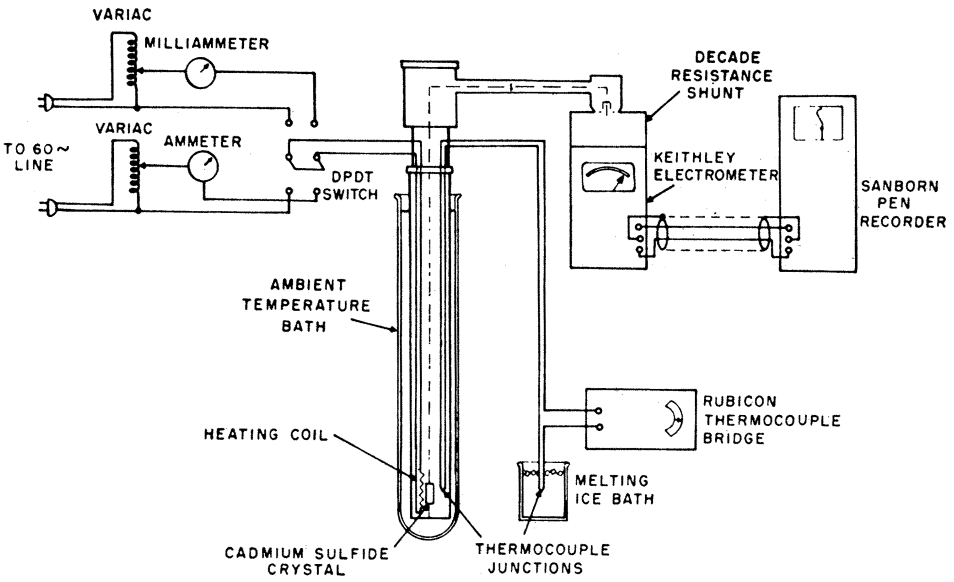

FIG. 1. Experimental equipment.

* This paper is based upon a Master of Science thesis submitted by the author to the Graduate School of Northwestern University. The work was sponsored by the Wright Air Development Center under Contract AF 33(616)-5625.
† The author is presently affiliated with the Rome Air Development Center, U. S. Air Force Systems Command.

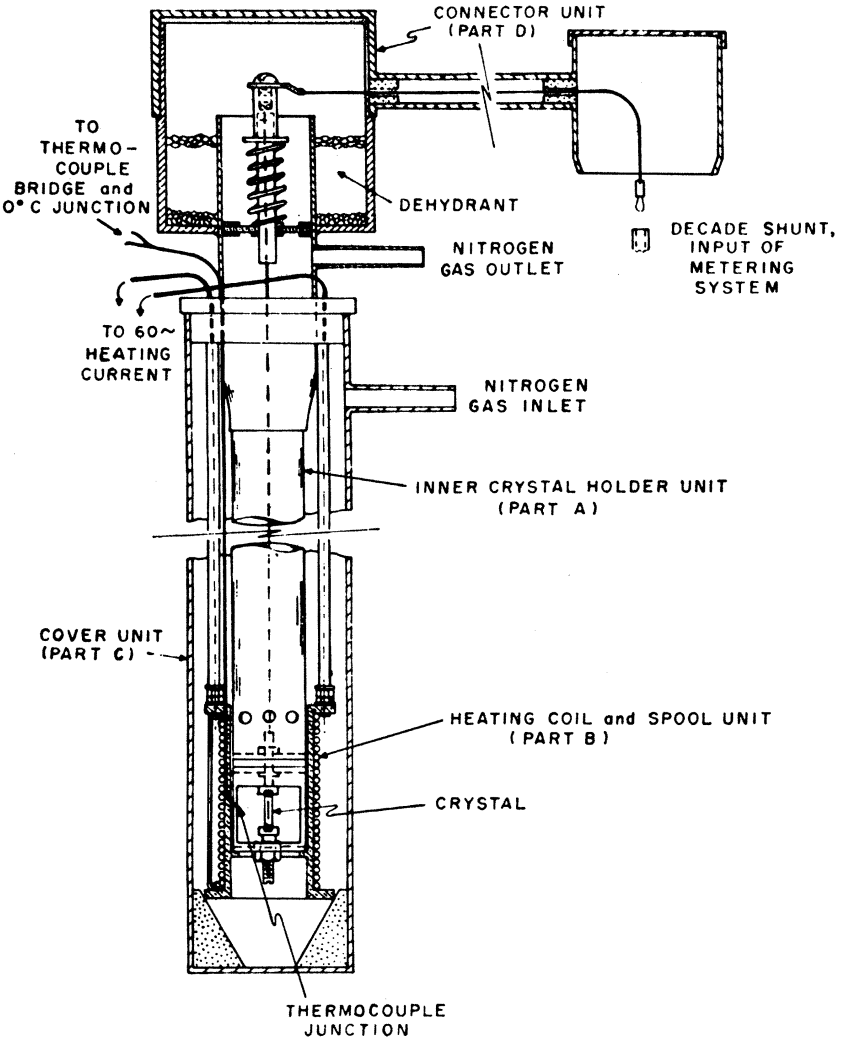

FIG. 2. Crystal holder.

with a junction set at an opening in its wall just opposite the crystal.

The inner holder and heating coil units were placed in a brass cylinder of 30-mm diameter that served as a cover. This unit enabled the holder to be immersed in the fluids that provided the constant ambient temperatures. The output of the holder was coupled to an amplifier through a shielded connector that also served as a light-tight lid. To prevent the insulation of the device from being deteriorated by moisture, a supply of a dehydrant was maintained in an annular region in the connector. As an additional precaution, a small amount of dry nitrogen was flushed through the holder when it was cooled or otherwise subject to condensation. Without the crystal in place and with its insulation intact, the conductance and capacitance measured at the output of the crystal holder were about 6.6×10^{-16} mho and 21 $\mu\mu$F.

The lower four-fifths of the crystal holder was immersed in a hot-water bath, room-temperature air, a melting-ice solution, a mixture of ice and salt, a mixture of dry ice and a special antifreeze, and liquid nitrogen. These provided the constant ambient temperatures of 345, 300, 273, 253, 195, and 78°K, respectively. The pyroelectric response was obtained by heating the crystal about 2.5 deg above the ambient. To heat the specimen quickly, a current of about 1.5 A was used for the first 4 to 5 sec, after which a current of 90 to 130 mA was used to maintain the crystal at a constant elevated temperature. A Rubicon thermocouple bridge was used to measure the ambient and the temperature rise of the specimen. One junction of the thermocouple was placed near the crystal, as indicated above, and the other was placed in a melting-ice solution. The current-switching and thermocouple circuits are shown in Fig. 1.

The crystal holder was connected to the input of a Keithley electrometer in parallel with a $1.01\times10^{12}\pm1\%$ resistor. The electrometer output was connected to a Sanborn recorder, where the pyroelectric response was recorded as a function of time. This combination served

as a dc amplifier and pen recorder with an exceptionally high and accurately known input resistance. The characteristics of the system were more than adequate for the relatively slow response presented to it. A typical recording made at room temperature is indicated in Fig. 3.

2. COMPUTING THE VALUES OF THE PYROELECTRIC CONSTANT

The parallel circuit representing the crystal, its holder, the 1.01×10^{12}-Ω shunt, and the electrometer input will be referred to as the input circuit in the discussion which follows. When the crystal is heated, the charge that is produced is stored by the capacitance of this circuit and leaks off through its conductance. The amount of charge that is produced is equal to the product of the time integral of the voltage appearing across the input circuit and its total conductance. The pyroelectric constant is obtained by dividing this amount by the effective cross-sectional area of the crystal and its temperature rise. It can be computed from the area of the recorded response curve as follows:

$$p=AG\lambda_1\lambda_2/B\Delta T, \quad (1)$$

where p is the pyroelectric constant, A is the area of the response curve, G is the total conductance of the input circuit, λ_1 is the deflection of the recorder per volt input at the electrometer, λ_2 is the number of seconds per unit length along the time base of the recording, B is the effective cross section of the specimen, and ΔT is its temperature rise.

Because the capacitance of the input circuit did not change significantly during the study, variations in the conductance G could be determined from time-constant measurements. In these tests a voltage source was placed across the electrometer input and the time constant was determined from the decay curve produced on the recorder when the source was removed. The conductance of the crystal varied in an exponential manner with temperature but, except at the 300 and 345°K ambients, it was insignificant compared with that of the shunt. When the insulation of the crystal holder was unimpaired by moisture, its conductance was also insignificant compared to that of the shunt. Under this condition and at the lower ambients, the conductance of the input circuit was the 9.90×10^{-13} mho value of the shunt. The time constant measured here was 36.0 sec. Under other conditions a smaller time constant τ was measured, and the conductance was determined as follows:

$$G=9.90\times10^{-13}\times36.0/\tau. \quad (2)$$

The conductivity of a cadmium sulfide crystal was investigated between 298 and 373°K and found to obey the following law[1]:

$$g=0.17\exp-(0.67/kT), \quad (3)$$

[1] R. Frerichs, Phys. Rev. **76**, 1869 (1949).

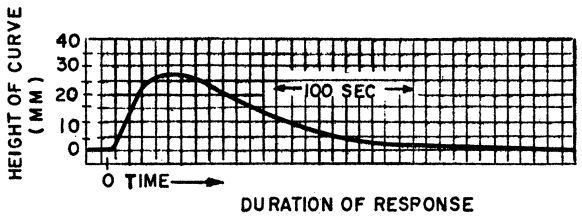

FIG. 3. Reproduction of a typical pyroelectric-response curve recorded at room temperature (300°K).

where g is the conductivity in mho meter^{-1}, k is Boltzmann's constant, and T is the absolute temperature. The effect of this temperature dependence was significant only at the 345°K ambient. Here the crystal contributes about half the total conductance of the input circuit, and when heated produces a small but noticeable increase in its value. The input conductance values that were determined from Eq. (2) had to be adjusted for this increase. The average adjustment in input conductance was 5.2%.

A few of the response curves were affected by electrometer drift. Instead of giving to zero at the end of the measurement, as indicated by the curve of Fig. 3, they settled to a level that was slightly above or below it. A correction was made for this effect.

3. THE RESULTS OF THE MEASUREMENTS

The values which were determined for the pyroelectric constant at each ambient temperature are indicated in Fig. 4. There were two general types of errors which affected the results. One type affected all the pyroelectric-constant values by the same percentage, while the other influenced them in an individual manner. The effect of the first of these was to shift the entire mean-pyroelectric-constant characteristic of Fig. 4 vertically without altering its shape. The absolute sum of errors of this type was 26%. The main contributor to this sum, and by far the largest source of error encountered in the study, was the 20% allowed for determining the effective cross-sectional area of the crystal. It occurred because the fragile condition of the specimen did not permit this area to be determined too accurately from its varying width and thickness dimensions.

This second type of error caused the individual values to deviate from their mean. Its effect can be expressed as a probable error by which the actual mean could deviate from its computed value. At each temperature, this error was computed as a rms-type average of the deviations of the individual values from their mean, and as a rms-type average of the errors affecting each factor in Eq. (1), from which the values of the pyroelectric constant were computed. The final magnitude of the probable error at each ambient is taken as the average of the corresponding values of the two computations. These values are indicated in Table I, where the result of the first computation is referred to as E_{p1} and that of the second as E_{p2}. The probable limits between which

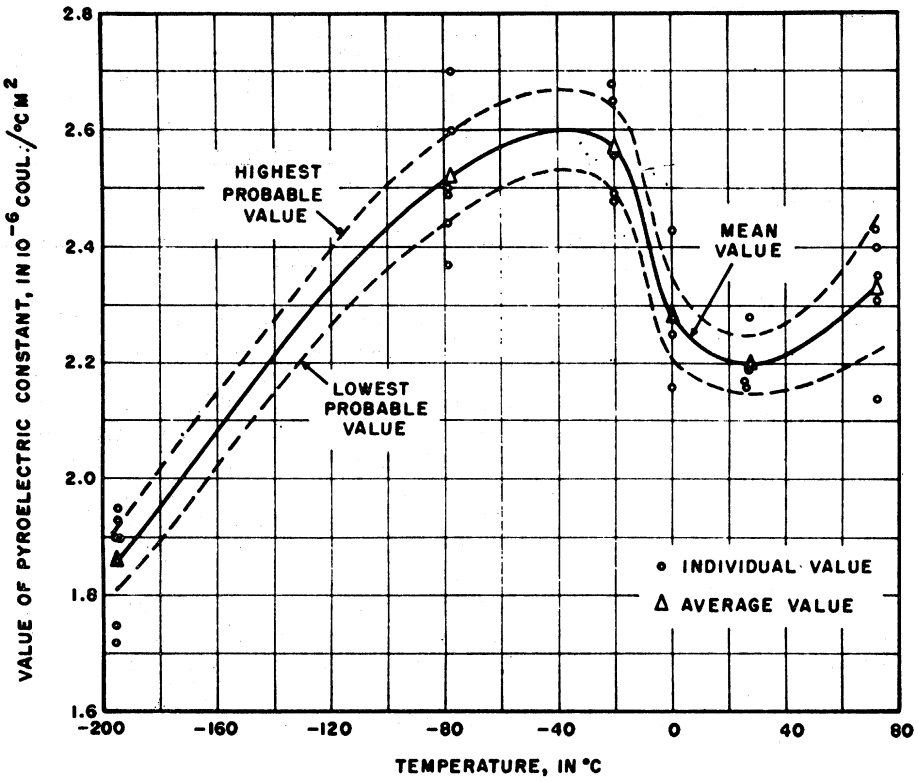

FIG. 4. Computed pyroelectric-constant values versus temperature.

the mean pyroelectric constant can vary are indicated in Table I and shown by the pair of dashed lines in Fig. 4. The narrow limits of this probable error verify that the trend indicated by the mean characteristic of this figure is substantially correct.

4. THE RELATIONSHIP OF THE PYROELECTRIC EFFECT TO THE CRYSTAL'S STRUCTURE AND THE TYPE OF BINDING BETWEEN ITS ATOMS

A molecular group is defined as the smallest repeatable array of atoms from which a crystal can be constructed. The groups are simply oriented with respect to each other and have identical physical properties throughout the specimen. Since a pyroelectric crystal cannot have a center of symmetry, its molecular group must be tetrahedral if it is to be a regular polyhedron. This is because "the tetrahedron is the only regular polyhedron involving nearest neighbors that has no center of symmetry."[2] The configuration of a tetrahedral group is indicated in Fig. 5. The atom located at the central portion of the figure is of the opposite electrovalence to those situated at the corners and forms a dipole with each of them. There is effectively only one atom of each type in the structure, as each of the corner atoms is shared with three other groups. In more complicated compounds the single atoms are replaced by assemblies of atoms.

TABLE I. Mean values of the pyroelectric constant and their probable experimental errors.

Mean ambient temperature T, °K	Probable experimental error E_{p1}	Probable experimental error E_{p2}	Mean probable experimental error $(E_{p1}+E_{p2})/2$	Average pyroelectric-constant value p and its probable limits 10^{-6} C/°K m^2
345	±4.2%	±5.0%	±4.6%	2.33±0.11
300	±1.5%	±2.7%	±2.1%	2.20±0.05
273	±3.3%	±3.0%	±3.2%	2.28±0.07
253	±2.4%	±3.3%	±2.8%	2.57±0.07
195	±3.1%	±2.5%	±2.8%	2.52±0.07
78	±3.2%	±2.3%	±2.8%	1.86±0.05

One of the dipoles of the group lies along the symmetry axis of the crystal and has a dipole moment which is directed opposite to the net amount of the three which are obliquely positioned with respect to it. The molecular groups of a pyroelectric crystal are oriented with respect to each other so that atoms (or assemblies) of opposite electrovalence lie directly above each other along the symmetry axis. The electrostatic forces that result flatten the group in this direction, so that the net moment of the obliquely oriented dipoles no longer balances that of the dipole situated along the axis. The electrostatic forces also produce a reorientation of the obliquely positioned dipoles in the presence of thermal expansion. When an unclamped crystal is heated the change in the configuration of the molecular group, and

[2] A. Von Hippel, *Dielectrics and Waves* (John Wiley & Sons, Inc., New York, 1954), p. 201.

the polarization generated by this change, can be represented as a superposition of that due to an equal expansion of all the dipoles and that due to this reorientation. The dipole reorientation manifests itself in the anisotropic expansion pattern of the crystal, as well as in its pyroelectric effect.

The pyroelectric effect also depends on the shape of the moment versus length characteristic applicable to the elementary dipole of the substance. For a substance whose interatomic binding is completely ionic, the characteristic is a straight ascending line, as indicated by curve I of Fig. 6. This is an ideal characteristic, as the binding of no substance is completely ionic. The binding can be regarded as being partially ionic and partially covalent. When there is a small amount of covalency present, the curve drops slightly below this line at first but returns to it with further increases in dipole length.[3,4] This deviation increases with the proportion of covalent binding present, but until a certain limit is reached, the curve returns to the ascending line; as in curves II, III, and IV of Fig. 6. Beyond this limit the curve rises to a maximum but falls gradually to zero with increasing dipole length,[5] as the atoms take back the electrons entering into the interatomic bond. This situation is indicated by curves V and VI, and corresponds to the behavior of a substance in which the covalent type bond predominates. The curves become flatter with increasing covalency, the abscissa being the characteristic of a completely homopolar substance.

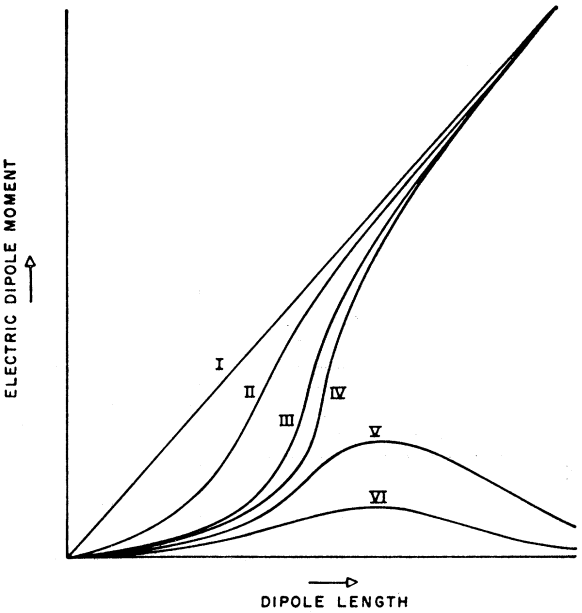

FIG. 6. Dipole moment versus dipole-length characteristics.

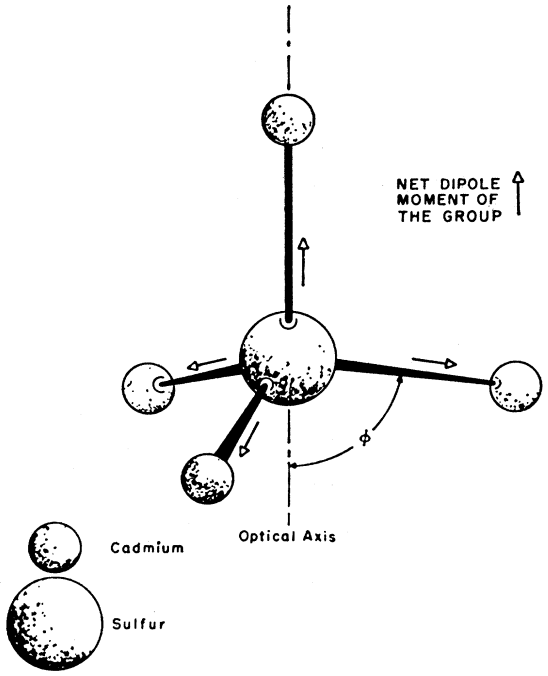

FIG. 5. Tetrahedral arrangement and dipole moments of the molecular group of hexagonal cadmium sulfide.

[3] E. Bartholome, Z. Physik. Chem. 23, 131 (1933).
[4] A. Eucken and A. Büchner, Z. Physik. Chem. 27, 321 (1934).
[5] See Ref. 2, p. 210.

5. EXPLAINING THE EXPERIMENTAL RESULTS

In the derivation that follows it will be assumed that the crystal is uniformly heated and that there are no external fields across it. It can be shown that errors that occur because of deviations from these conditions are negligible. If it is assumed that the interatomic binding between dipole pairs that produce the dominant contribution of polarization is principally covalent, the dipole moment versus dipole length characteristic is similar to curve V of Fig. 6. This curve is reproduced in Fig. 7 and will be used in the analysis.

At the beginning of the measurement, the crystal is at the ambient temperature T and is electrically neutral at its surface. The molecular group has a net dipole moment which is the difference between the moment of the dipole aligned along the crystal's symmetry (and optical) axis and the net moment of the three dipoles which are obliquely oriented with respect to it. Referring to Figs. 5 and 7, this can be expressed as follows:

$$M_{g0}=M_0(1-3\cos\varphi_0)=k_0D_0(1-3\cos\varphi_0), \quad (4)$$

where M_{g0} is the dipole moment of the group, M_0 is the moment of each dipole, D_0 is the dipole length, φ_0 is the angle between the symmetry axis and each obliquely oriented dipole, and $k_0=M_0/D_0$.

When the temperature of the crystal changes by a small amount ΔT, the dipole moment of the molecular

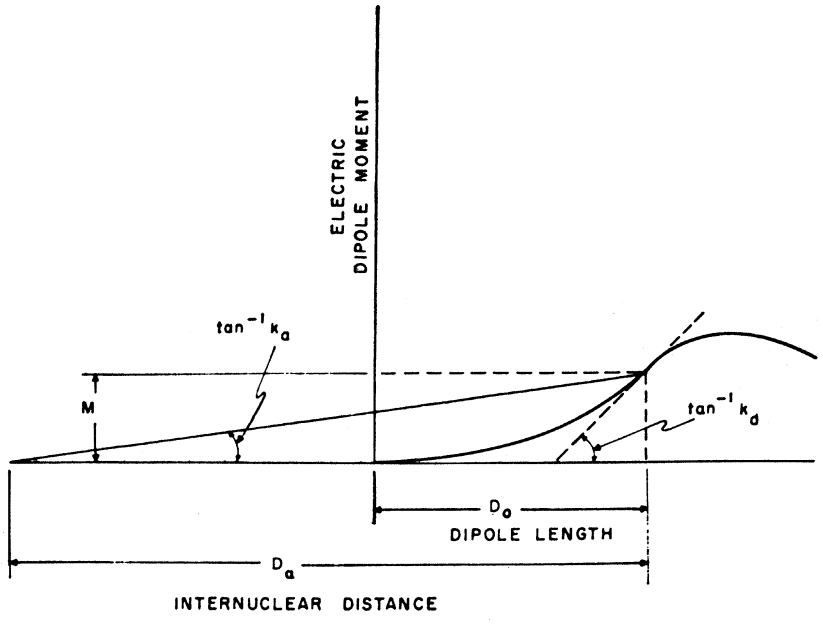

FIG. 7. Dipole moment versus dipole-length characteristic of the type applicable to hexagonal cadmium sulfide.

group changes to M_{g1}, where

$$M_{g1}=D_0(k_0+\delta_d k_d)[1-3\cos(\varphi_0+\delta_r\varphi_0)]$$
$$\doteq M_{g0}+k_d\delta_d D_0(1-3\cos\varphi_0)-3k_0D_0\delta_r\varphi_0\sin\varphi_0,$$
$$\text{for}\quad \delta_r\varphi_0\ll 1, \quad (5)$$

where δ_d and δ_r are the proportional changes in D_0 and φ_0, respectively, and k_d is the slope of the dipole moment versus dipole length characteristic.

As a first order approximation the electrical polarization of the atom is independent of temperature.[6] This means that the dipole length and the distance between the nuclei of the dipole partners change by the same amount when the temperature is changed. This relationship can be expressed as follows:

$$\delta_d D_0=\delta_a D_a, \quad (6)$$

where D_a is the internuclear distance and δ_a is its proportional change. On letting $k_a=M_0/D_a$, we also have that

$$k_0D_0=k_aD_a. \quad (7)$$

δ_a obeys a linear expansion law. For such a condition it has a temperature dependence similar to that of the specific heat at constant volume (except near 0°K).[7] This permits the following relation to be written

$$\delta_a(T)=\Delta T\alpha_a C(T), \quad (8)$$

where $\delta_a(T)$ is δ_a evaluated at temperature T, α_a is the value of δ_a per degree temperature change at temperature T_0, and $C(T)$ is the ratio of the specific heat at constant volume at temperature T to that at T_0. The specific heat was evaluated from a handbook.[8] The Debye characteristic temperature of zinc sulfide, 300°K, was used as an approximation in this evaluation. The value of T_0 was set equal to 345°K, the highest ambient used in the study. This made $C(T)$ a normalized quantity. The values of $C(T)$ that were determined are indicated in Table II, which follows. α_a is evaluated in Appendix A.

The total polarization produced by the heated crystal is equal to the product of the change in the dipole moment of each molecular group and the number of such groups per unit volume of the crystal. Denoting the latter quantity as N_c and using Eqs. (5), (6), (7), and (8), the following expression is obtained for the total polarization, $\Delta P(T)$:

$$\Delta P(T)=N_c(M_{g1}-M_{g0})$$
$$\doteq N_c\Delta T D_a\alpha_a C(T)[k_d(T)(1-3\cos\varphi_0)$$
$$-3k_a(T)(\delta_r/\delta_a)\varphi_0\sin\varphi_0]. \quad (9)$$

The quantities which are temperature-dependent in Eq. (9) are indicated by the functional notation. The proportional changes in D_a and φ_0 are so small over the entire temperature range of the study, that they are regarded as constants here. As will be shown in Appendix A, this same situation applies to the ratio (δ_r/δ_a). Since the pyroelectric constant is defined as the polarization produced per degree temperature change of the crystal, its expression is obtained by dividing Eq. (9) by ΔT. The result is

$$p(T)=\Delta P(T)/\Delta T\doteq N_cD_a\alpha_a C(T)$$
$$\times[k_d(T)(1-3\cos\varphi_0)-3k_a(T)\epsilon\varphi_0\sin\varphi_0], \quad (10)$$

[6] Y. K. Syrkin and M. E. Dyatkina, *Structure of Molecules and the Chemical Bond*, translated and revised by M. A. Partridge and D. O. Jordan (Interscience Publishers, Inc., New York, 1950), p. 193.

[7] C. Zwikker, *Physical Properties of Solid Materials* (Interscience Publishers, Inc., New York, 1954), pp. 153–157.

[8] *American Institute of Physics Handbook* (McGraw-Hill Book Company, Inc., New York, 1957), p. 4–44.

TABLE II. Values computed for temperature-dependent parameters.

T °K	$C(T)$	$\Delta D_a(T)$ 10^{-14} m	$M(T)$ 10^{-30} C m	$k_d(T)$ 10^{-18} C	$k_a(T)$ 10^{-20} C	$p_I(T)$ C 10^{-6} ——— °K m²	$p_{II}(T)$ C 10^{-6} ——— °K m²	$p(T)$ C 10^{-6} ——— °K m²
345	1.00	34.72	4.63	3.55	1.83	1.64	0.596	2.24
300	0.990	28.36	4.40	3.61	1.74	1.66	0.561	2.22
273	0.979	24.59	4.23	3.84	1.67	1.75	0.534	2.28
253	0.970	21.82	4.12	4.57	1.63	2.05	0.516	2.57
195	0.927	14.01	3.76	4.82	1.48	2.07	0.448	2.52
78	0.759	0	3.23	4.38	1.28	1.54	0.315	1.86

where $p(T)$ is the pyroelectric constant, and $\epsilon = (\delta_r/\delta_a)$, a constant.

The constants of Eq. (10) are evaluated in Appendix A. Using these values, the final result is expressed as follows:

$$p(T) \doteq 4.64 \times 10^{11} C(T)[k_d(T) + 70.2 k_a(T)]. \quad (11)$$

The values of $k_a(T)$ and $k_d(T)$ are determined by the method indicated in Appendix B. The method of determining $M(T)$, the moment of the elementary cadmium sulfide dipole, is also presented here; as is the means of determining $\Delta D_a(T)$, the change that occurs in its internuclear distance as the ambient temperature

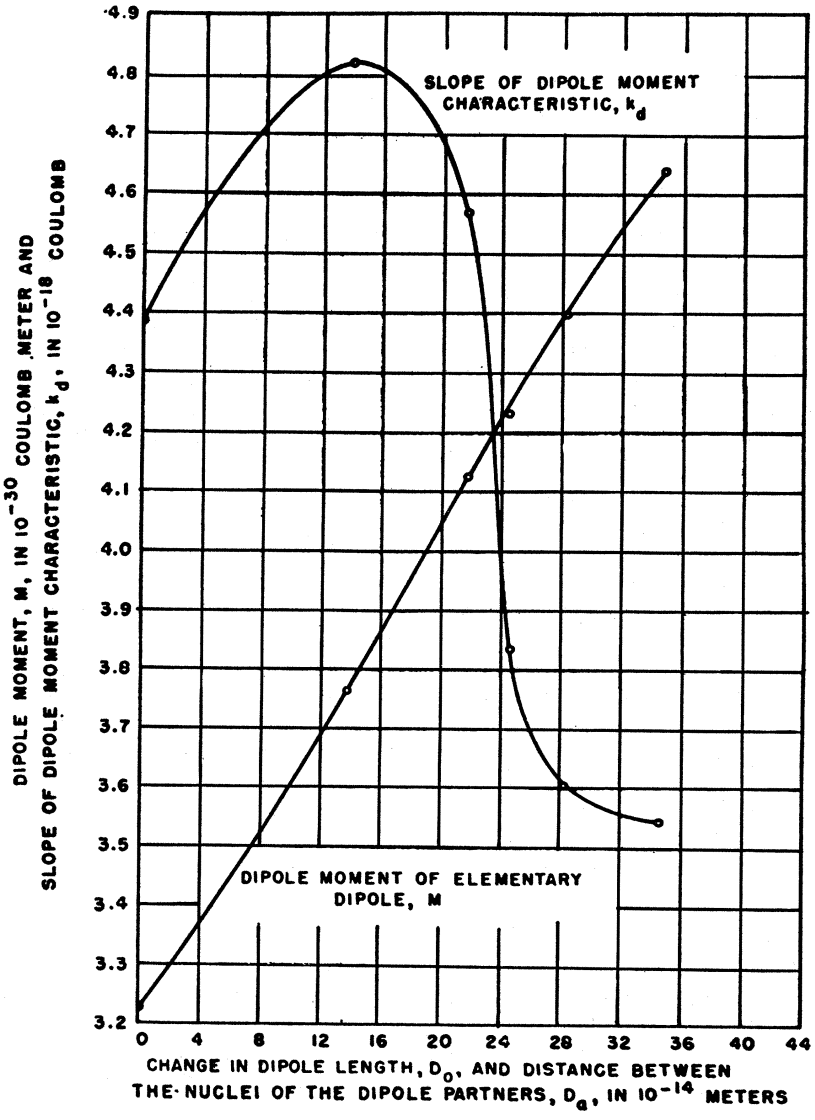

FIG. 8. Values of the moment and the slope of the moment versus length characteristic as computed for the elementary cadmium sulfide dipole.

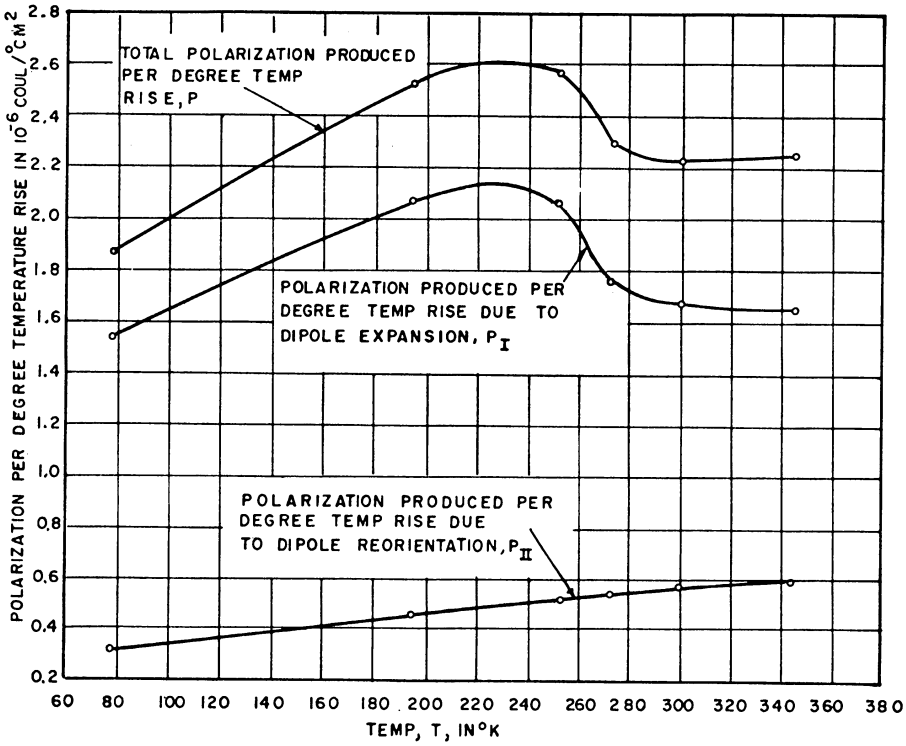

FIG. 9. Components of polarization produced by the pyroelectric effect.

is increased from its lowest value of 78°K. The values that were determined for these quantities at each ambient are indicated in Table II, and the characteristics of $k_d(T)$ and $M(T)$ versus $\Delta D_a(T)$ are presented in Fig. 8. Since, as is indicated in Eq. (6), the change in dipole length is equal to the change in internuclear distance, the curves of Fig. 8 are also presented as a function of this quantity.

The first and second right-hand terms of Eq. (11) represent, respectively, the polarization produced per degree temperature rise due to dipole expansion, $P_I(T)$; and that due to dipole reorientation, $P_{II}(T)$. The values which were determined for these components and that of their sum, the pyroelectric constant, are added to Table II and indicated in Fig. 9. Figure 9 shows that, throughout the temperature range of this study, the dominant contribution of polarization is produced by dipole expansion. From 78 to 300°K the shape of the pyroelectric constant versus temperature characteristic is almost entirely determined by it. Above 300°K the polarization due to dipole reorientation starts to become significant. It is responsible for the rise in the value of the pyroelectric constant that occurs between 300 and 345°K.

6. SUMMARY

The values of the pyroelectric constant that were obtained at each of the ambient temperatures are indicated in Fig. 4. The probable limits in which the mean values lie are shown here and indicated in Table I. These limits are narrow enough so that the shape of the mean characteristic of Fig. 4 can be assumed to be substantially correct.

The dipole moment versus dipole length characteristic changes from an ascending curve to one that rises to a maximum and then falls to zero as the interatomic binding of the pair producing the polarization changes from being predominantly ionic to predominantly covalent. The slope of the characteristic applicable to cadmium sulfide has been computed over the dipole lengths corresponding to the temperature range of the measurements and is shown in Fig. 8. It is seen that these slopes correspond to those that would be found about the inflection point of a dipole moment versus dipole length characteristic associated with predominantly covalent binding.

The simplest array of atoms from which the crystal can be constructed is termed the molecular group. For the group of a pyroelectric crystal to be of geometric regularity requires that it be of tetrahedral configuration. Electrostatic forces acting along the symmetry axis of the crystal flatten the configuration, causing the group to have a net dipole moment in this direction. When the crystal is heated this net moment changes. The polarization that is produced is considered to be due to an equal expansion of all the dipoles and to a reorientation of those which are obliquely positioned with respect to the symmetry axis. The amount produced by the expansion is proportional to $k_d(T)$, the slope of the dipole moment versus dipole length characteristic; while that due to the reorientation is proportional to $k_a(T)$,

which depends on the height of this curve. This is clearly indicated in Eq. (11), where it is also shown that both of these components are proportional to $C(T)$, the normalized specific heat at constant volume. The amounts of polarization contributed by these two effects were computed over the temperature range of the study. These results are presented in Table II. They show that over this range the dominant amount of polarization is due to dipole expansion.

ACKNOWLEDGMENT

The author wishes to express his sincere appreciation to Dr. R. Frerichs for the assistance and guidance he gave throughout the course of the investigation.

APPENDIXES

The constants of Eq. (10) are evaluated in Appendix A, and the methods for determining the values of its temperature dependent parameters are indicated in Appendix B. Except for the few which will be described here, the symbols which are used have been defined in the discussion associated with the development of Eqs. (4) through (10).

Appendix A

The projection of the tetrahedral structure of a molecular group and two of its nearest neighbors on a plane perpendicular to the symmetry (and the optical) axis of the crystal is indicated in Fig. 10. It is seen that the projected area of a molecular group is an equilateral triangle whose side length is equal to the crystallographic dimension "a," and that the projected area between two adjacent groups is equal to that of a group. With the height of the group perpendicular to the projection plane equal to the crystallographic dimension "c," the volume required by each group in the crystal, including the space between groups, is $1/N_c$, where

$$1/N_c=(c/2)(a^2\cos 30°). \tag{A1}$$

The crystallographic dimensions a and c have been evaluated as 4.142×10^{-10} and 6.724×10^{-10} m, respectively.[9] Using these values yields

$$N_c=2.002\times10^{28}\ \text{groups/m}^3.$$

From Figs. 5 and 10 it is seen that

$$H_0=D_a(1+\cos\varphi_0)=c/2=3.362\times10^{-10}\ \text{m}, \tag{A2}$$

$$J_0=D_a\sin\varphi_0=(a/2)\sec 30°=2.391\times10^{-10}\ \text{m}, \tag{A3}$$

where H_0 is the height of the molecular group perpendicular to the projection plane, and J_0 is the projection on the plane of the distance D_a of an obliquely oriented pair of dipole partners.

[9] P. P. Ewald and C. Hermann, *Zeitschrift für Kristallographie, Ergänzungsband, Strukturbericht*, (1913–1928), Vol. 1, p. 129.

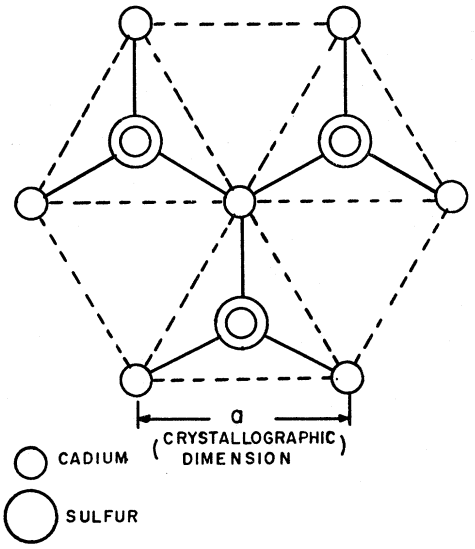

FIG. 10. Projection of three neighboring molecular groups of hexagonal cadmium sulfide on a plane perpendicular to the axis of symmetry of the crystal.

Dividing Eq. (A2) by (A3) and solving for φ_0 yields

$$\varphi_0=70°\ 51.5'=1.237\ \text{rad}.$$

Using this value in Eq. (A3) yields

$$D_a=2.531\times10^{-10}\ \text{m}.$$

When the temperature changes by a small amount ΔT, H_0 changes to H_1, where

$$H_1=D_a(1+\delta_a)[1+\cos(\varphi_0+\delta_r\varphi_0)]$$
$$\doteq H_0+D_a\delta_a(1+\cos\varphi_0)-D_a\delta_r\varphi_0\sin\varphi_0,$$
$$\text{for}\quad \delta_r\varphi_0\ll1. \tag{A4}$$

Using Eqs. (A2) and (A4), the following expression is obtained for the coefficient of thermal expansion parallel to the symmetry axis, $\alpha_{\parallel}$:

$$\Delta T\alpha_{\parallel}=(H_1-H_0)/H_0$$
$$\doteq\delta_a-(\delta_r\varphi_0\sin\varphi_0)/(1+\cos\varphi_0). \tag{A5}$$

Using this same procedure for the change in J_0 with ΔT, the following expression is obtained for the coefficient of thermal expansion perpendicular to the symmetry axis, $\alpha_{\perp}$:

$$\Delta T\alpha_{\perp}\doteq\delta_a+\delta_r\varphi_0\cot\varphi_0. \tag{A6}$$

Dividing Eq. (A6) by (A5), simplifying, and solving for $\epsilon=\delta_r/\delta_a$ yields

$$\epsilon\doteq\frac{(\alpha_{\perp}/\alpha_{\parallel}-1)\tan\varphi_0}{\varphi_0[1+(\alpha_{\perp}/\alpha_{\parallel})(\sec\varphi_0-1)]}. \tag{A7}$$

Subtracting Eq. (A5) from (A6), simplifying, and solving for $(\delta_r/\Delta T)$ yields

$$(\delta_r/\Delta T)\doteq[(\alpha_{\perp}-\alpha_{\parallel})\sin\varphi_0]/\varphi_0. \tag{A8}$$

The change in φ_0 is so small over the temperature range of this study that it can be regarded as a constant equal to the value computed above. $\alpha_\perp$ and $\alpha_{||}$ have been measured between 290 and 960°K.[10] The results indicated that, for practical purposes, $\alpha_\perp$ and $\alpha_{||}$ are constant at about 6.4×10^{-6} and 4.0×10^{-6} per degree, respectively, between 290 and 510°K; and that the ratio between them is constant over the entire range. It is interesting to note that where $\alpha_\perp$ and $\alpha_{||}$ have been measured more extensively, as they have been for quartz, the ratio between them appears to be nearly constant.[11,12] If it is assumed, for computational purposes, that $\alpha_\perp$ and $\alpha_{||}$ are exactly equal to the indicated values at the temperature $T_0=345$°K and that $\alpha_\perp/\alpha_{||}$ is exactly equal to 1.6 at all temperatures, then, using the computed value of φ_0, Eqs. (A7) and (A8) can be evaluated as follows:

$$\epsilon\doteq0.327, \text{ for all temperatures,}$$

$$(\delta_r/\Delta T)T_0\doteq1.83\times10^{-6} \text{ per degree, for } T_0=345°\text{K.}$$

As $\alpha_a=(\delta_a/\Delta T)_{T_0}\doteq(1/\epsilon)(\delta_r/\Delta T)_{T_0}$, we also have that

$$\alpha_a\doteq5.60\times10^{-6} \text{ per degree.}$$

Appendix B

Equation (6) indicates that D_a and D_0 change by the same amount when the temperature is varied. Using this fact and referring to Fig. 7, the following expression is obtained for the differential change in the moment of an elementary dipole:

$$d[M(T)]=k_d(T)d[D_0(T)]=k_d(T)d[D_a(T)]. \quad \text{(B1)}$$

With the aid of the definition of $k_a(T)$ indicated at Eq. (7) and that of α_a indicated at Eq. (8), it is seen that

$$d[k_a(T)]=d[M(T)/D_a(T)]\doteq d[M(T)]/D_a(T), \quad \text{for } d[D_a]/D_a\ll d[M]/M, \quad \text{(B2)}$$

$$C(T)\alpha_aD_a(T)dT=d[D_a(T)]. \quad \text{(B3)}$$

Using Eqs. (B1), (B2), (B3), the following expression is obtained:

$$d[k_a(T)]\doteq\alpha_ak_d(T)C(T)dT. \quad \text{(B4)}$$

α_a is a constant. The temperature variations in $C(T)$ and $k_d(T)$ are such that they can be approximated as linear functions between adjacent ambients. Designating the ambient temperatures as T_n, where $T_n<T_{n-1}$ and $T_0=345$°K, the following expression is obtained from Eq. (B4):

$$\int_{T_{n-1}}^{T_n}d[k_a(T)]\doteq(\alpha_a/2)\times[k_d(T_n)C(T_n)+k_d(T_{n-1})C(T_{n-1})]\int_{T_{n-1}}^{T_n}dT.$$

From which

$$k_a(T_n)\doteq k_a(T_{n-1})-(\alpha_a/2)[k_d(T_n)C(T_n)+k_d(T_{n-1})C(T_{n-1})][T_{n-1}-T_n]. \quad \text{(B5)}$$

Using the T_n notation in Eq. (11), and substituting Eq. (B5) into it yields

$$p(T_n)\doteq4.64\times10^{11}C(T_n)\{k_d(T_n)+70.2k_a(T_{n-1})-35.1\alpha_a[k_d(T_n)C(T_n)+k_d(T_{n-1})C(T_{n-1})][T_{n-1}-T_n]\}. \quad \text{(B6)}$$

Letting

$$Q(T_n)=p(T_n)/[4.64\times10^{11}C(T_n)],$$

$$K(T_n)=35.1\alpha_ak_d(T_{n-1})C(T_{n-1})[T_{n-1}-T_n],$$

$$L(T_n)=35.1\alpha_aC(T_n)[T_{n-1}-T_n],$$

the following expression is obtained from Eq. (B6):

$$k_d(T_n)\doteq[Q(T_n)+K(T_n)-70.2k_a(T_{n-1})]/[1-L(T_n)], \quad \text{(B7)}$$

and the following expression is obtained from Eq. (11):

$$k_a(T_n)\doteq[Q(T_n)-k_d(T_n)]/70.2. \quad \text{(B8)}$$

The value of α_a, required in the above equations, is indicated in Appendix A. Except at $T_0=345$°K and $T_1=300$°K, $p(T_n)$ is evaluated at the mean values indicated in Table I. $p(T_0)$ is evaluated at its mean minus (9/11)ths of its probable error, as shown in Table I; and $p(T_1)$ is evaluated at its mean plus (2/5)ths of its probable error. The values of $C(T_n)$ are determined using the procedure indicated in the discussion following Eq. (8). The values of $p(T_n)$ and $C(T_n)$ are indicated in Table II. If a value of either $k_d(T_n)$ or $k_a(T_n)$ were known at one temperature, it would be possible to compute their values at the other ambients used in the study by using Eqs. (B7) and (B8). To find this one value is the next step of the calculation procedure.

The dipole moments and internuclear distances of carbon fluoride, carbon chloride, carbon bromide, and carbon iodide have been determined.[13] Although the number of electrons entering into each of these carbon halogen bonds is twice that of cadmium sulfide, the covalency and internuclear distance of these bonds are similar to those of the cadmium sulfide bond. As an approximation, the value of $k_a(T_0)$ is set equal to the average ratio of the dipole moment to the internuclear distance of these compounds. The evaluation is made at $T_0=345$°K for convenience of calculation. The value of $k_d(T_0)$ is evaluated from Eq. (B8), and the values of $k_d(T_n)$ and $k_a(T_n)$ at the other ambient temperatures are then alternately computed using Eqs. (B7) and (B8).

[10] R. Seiwert, Ann. Physik **6**, 241 (1949).
[11] C. L. Lindermann, Z. Physik. **13**, 737 (1912).
[12] A. H. Jay, Proc. Roy. Soc. (London) **A142**, 237 (1933).
[13] See Ref. 6, p. 215.

The internuclear distance between dipole partners expands as the temperature is increased. By approximating $C(T_n)$ as a linear function between adjacent ambients, $\Delta D_a(T_n)$, the change that occurs in this distance as the ambient is increased from its lowest value of 78°K to T_n can be expressed as follows:

$$\Delta D_a(T_n)=(\alpha_a/2)\sum_{m=n}^{4}[C(T_m)+C(T_{m+1})][T_m-T_{m+1}],$$

$$\text{for } n=0,1,2,3,4 \text{ and } T_{m+1}<T_m. \quad \text{(B9)}$$

The results of Eq. (B9) show that the change in the internuclear distance D_a is so small over the entire temperature range of the study that it can be regarded as a constant. Using the value of D_a computed in Appendix A, the moment of an elementary cadmium sulfide dipole at temperature T_n can be expressed as follows:

$$M(T_n)=D_a k_a(T_n). \quad \text{(B10)}$$

The values that were obtained for $k_d(T_n)$, $k_a(T_n)$, $\Delta D_a(T_n)$, and $M(T_n)$ are indicated in Table II.

PHYSICAL REVIEW VOLUME 138, NUMBER 4A 17 MAY 1965

Optically Induced Magnetization in Ruby*

J. P. VAN DER ZIEL
Division of Engineering and Applied Physics, Harvard University, Cambridge, Massachusetts

AND

N. BLOEMBERGEN†
Department of Physics, University of California, Berkeley, California

(Received 21 December 1964)

The magnetization of ruby in a magnetic field at 300°K is changed when the ruby is optically pumped with linearly polarized radiation from a Q-switched ruby laser. With a magnetic field parallel to the trigonal axis, laser light polarized parallel to this axis induces transitions from the spin $\pm\frac{1}{2}$ levels of the $^4A_2$ ground state to the levels of the $\bar{E}(^2E)$ excited state. The change in M_z is linearly proportional to H except near the anticrossing points of the $^4A_2$ spin levels at 2.07 and 4.14 kG. At these field strengths, there is an enhancement of the magnetization caused by state mixing of the $^4A_2$ wave functions. When H has a small component perpendicular to the z axis, a magnetization is detected parallel to this component in the vicinity of 4.14 kG. The effect requires a long ground-state relaxation time. In a separate experiment, the relaxation of M_z was found to vary from 0.13 μsec in zero magnetic field to a constant value of 0.57 μsec for fields above 60 G.

1. INTRODUCTION

LINEARLY polarized radiation from a Q-switched ruby laser has been used to optically pump a ruby crystal. When the crystal is in a magnetic field, the changes in population of the energy levels $^4A_2$, $\bar{E}$, and $2\bar{A}$ of the chromium ions cause a change in the magnetization. Expressions for the field dependence of the magnetization are obtained in Sec. 2 for the case that both the laser polarization and the magnetic field are parallel to the optic axis. The experimental results discussed in Sec. 3 show the solid-state analog of anticrossing-state mixing experiments in gases and indicate that the relaxation time of the ground state is long compared to the laser pulse length. Quantitative measurements of the relaxation rate in small magnetic fields, using circularly polarized laser radiation, are reported in Sec. 4.

* This work was supported in part by the Joint Services Electronics Program under Contract Nonr-1866(16), and by the Division of Engineering and Applied Physics, Harvard University.

† On leave from Harvard University, Cambridge, Massachusetts.

2. THEORY

The splitting of the $^4A_2$, $\bar{E}$, and $2\bar{A}$ energy levels of ruby in a magnetic field parallel to the optic axis is shown Fig. 1. The ground state, with an effective spin of $\frac{3}{2}$, is described by the spin Hamiltonian[1]

$$\mathcal{H}=g_{\parallel}(^4A_2)\beta H\cos\theta S_z-D[S_z^2-\tfrac{1}{3}S(S+1)]$$
$$+\tfrac{1}{2}g_{\perp}(^4A_2)\beta H\sin\theta[e^{-i\varphi}S_+ + e^{+i\varphi}S_-]. \quad (1)$$

The g values are given in Table I, and the zero field splitting $2D$ is 0.3824 cm^{-1}. The magnetic field makes

TABLE I. The g values of Cr^{3+} in Al_2O_3.

Energy level	$g_{\parallel}$	$g_{\perp}$
$^4A_2$	1.9840±0.0006[a]	1.9867±0.0006[a]
$\bar{E}(^2E)$	−2.445 ±0.001[b]	<0.2[c]
$2\bar{A}(^2E)$	1.48 ±0.08[d]	...

[a] Reference 1. [b] Reference 4. [c] References 4 and 5. [d] Reference 6.

[1] A. A. Manenkov and A. M. Prokhorov, Zh. Eksperim. i Teor. Fiz. 28, 762 (1955) [English transl.: Soviet Phys.—JETP 1, 611 (1955)]; J. E. Geusic, Phys. Rev. 102, 1252 (1956).